

Supporting information:

## Characterization of the regrowth behavior of amyloid-like fragmented fibrils decomposed by ultrasonic treatment

Wonseok Lee,<sup>‡a</sup> Huihun Jung,<sup>‡b</sup> Myeonggu Son,<sup>a</sup> Hyungbeen Lee,<sup>a</sup> Tae Joon Kwak,<sup>a</sup> Gyudo Lee,<sup>a</sup> Chi Hyun Kim,<sup>a</sup> Sang Woo Lee<sup>a</sup> and Dae Sung Yoon\*<sup>c</sup>

<sup>a</sup> Department of Biomedical Engineering, Yonsei University, Wonju 220-710, Republic of Korea.

<sup>b</sup> Department of Engineering Science and Mechanics, Pennsylvania State University, PA, USA

<sup>c</sup> School of Biomedical Engineering, Korea University, Seoul 137-701, Republic of Korea.

<sup>‡</sup>These authors made equal contribution to this work.

\*Correspondence should be addressed to D. S. Yoon. (E-mail: dsyoon@korea.ac.kr)

### Preparation of $\beta$ -lactoglobulin fibrils and AFM imaging.

$\beta$ -lactoglobulin ( $\beta$ -lg) fibrils synthesized by using method of previous studies.<sup>1</sup>  $\beta$ -lg protein powder was purchased from Sigma Aldrich (USA). Protein powder was dissolved in buffer solution at pH 2 (titrated by hydrogen chloride solution, 10 M) so that the concentration of  $\beta$ -lg monomer was adjusted to 1 wt%. The solution was centrifuged at 20,000 rpm for 15 min and then its supernatant was filtered through a 0.22  $\mu$ m Millipore filter. Subsequently, the filtered solution was distributed in 25 ml vial, hermetically sealed, and heated at 90 °C for 10 h in oil bath. After heating, the amyloid solution was quenched in ice water for 3 min. The  $\beta$ -lg fibril solution was diluted to 0.1 wt% and then deposited on a clean glass disk for 1 min. The disk coated with  $\beta$ -lg fibrils was washed with pH 2 solution three times and gently dried by using a nitrogen gun. AFM images for analysis of the synthetic fibrils were acquired using a Multimode V (Veeco, USA) operated in tapping mode in air. The length distribution of  $\beta$ -lg fibrils was quantitatively measured and analyzed with the image program (i-Solution DT, IMT i-solution, Canada).

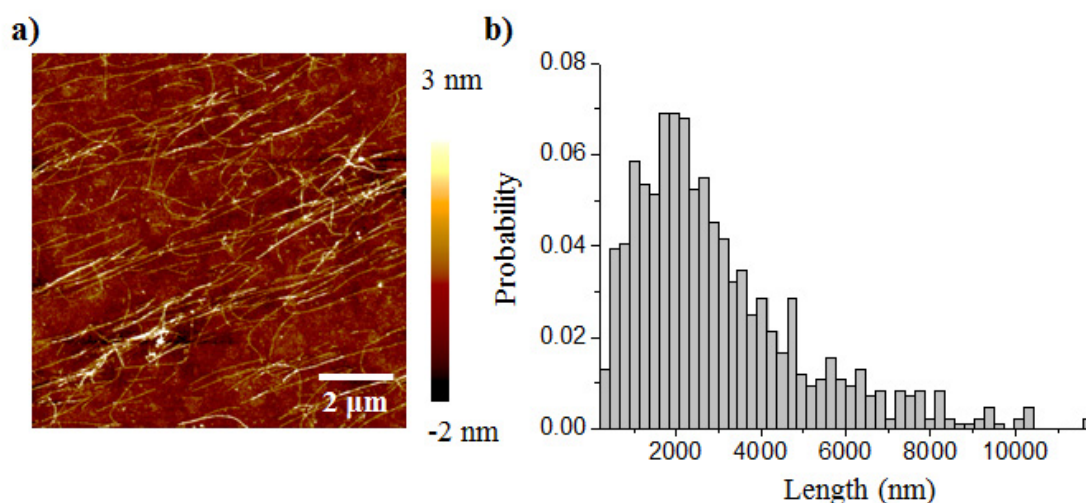


**Figure S1. AFM image and histogram of  $\beta$ -lactoglobulin fibrils. a)** AFM image of  $\beta$ -lactoglobulin fibrils (image size  $10 \times 10 \mu\text{m}^2$ ). **b)** The histogram of  $\beta$ -lactoglobulin fibrils.

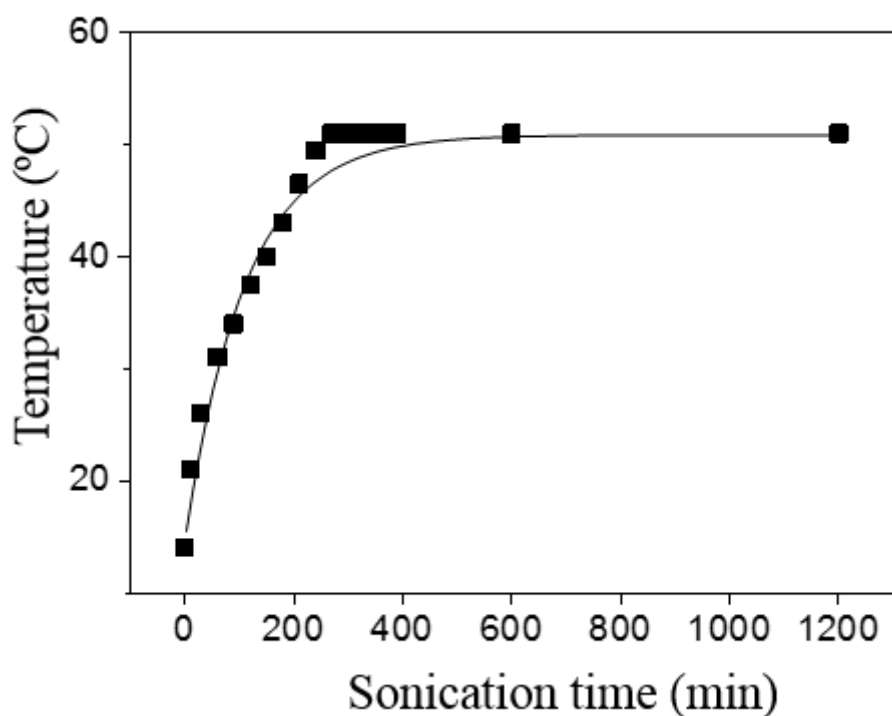


**Figure S2. Temperature variation of the solution with respect to the irradiation time of ultrasonic energy.** The solution temperature rapidly rises up at the initial stage and then its rate slows down with time. Finally, a plateau of the temperature after 300 min is observed. That is because the solution reaches a thermal equilibrium that is established by a balance between the heat generation and the thermal dissipation outward the bath. After the equilibrium state was reached, the ultrasonic energy was irradiated continuously into the fibril solution for time periods varying from 30 to 1,200 min.

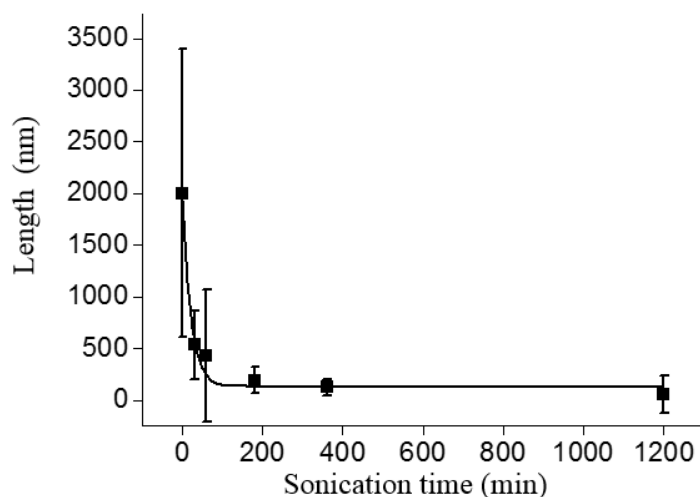


**Figure S3. Length variation of the decomposed fibrils with respect to the irradiation time of ultrasonic energy.** The fibril length was exponentially decreased with sonication time (see Figure 1).

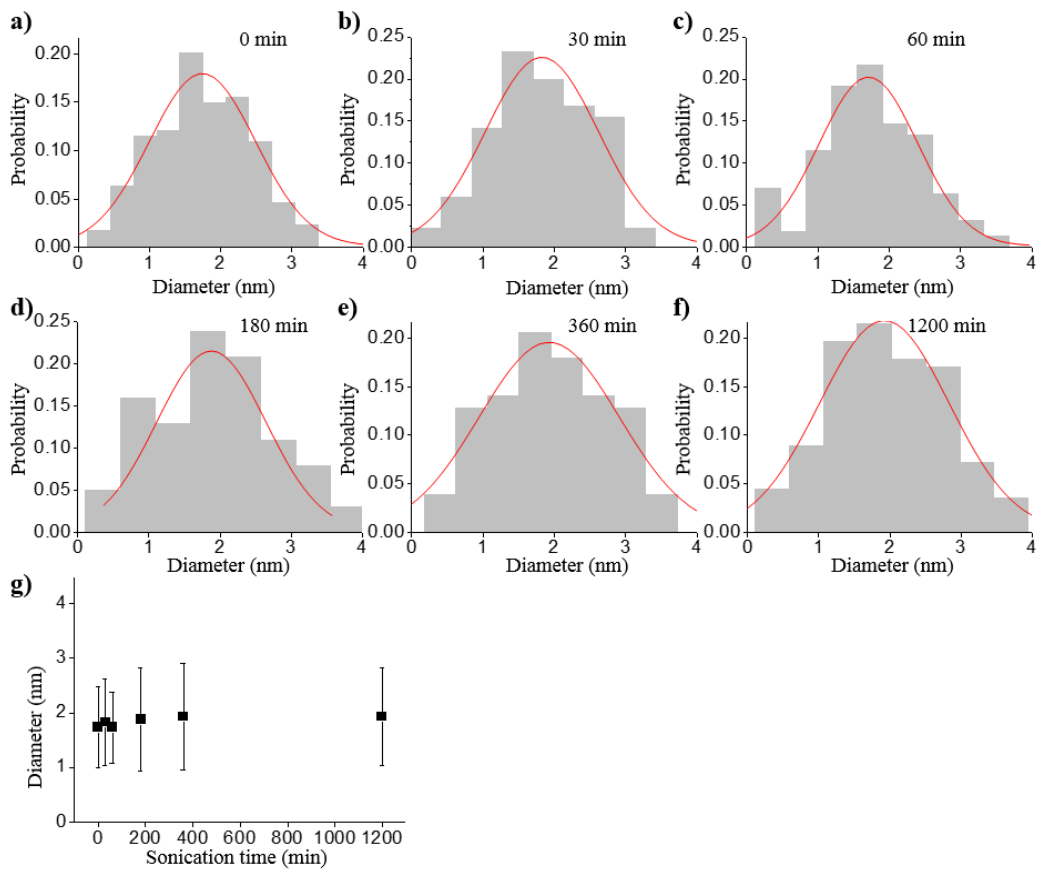


**Figure S4. Histogram of the fibril diameter distribution with respect to the irradiation time of UST. a-f) Histogram of the fibril diameter distribution depending on the irradiation time. g) Average diameters of fibrils with respect to the irradiation time.**

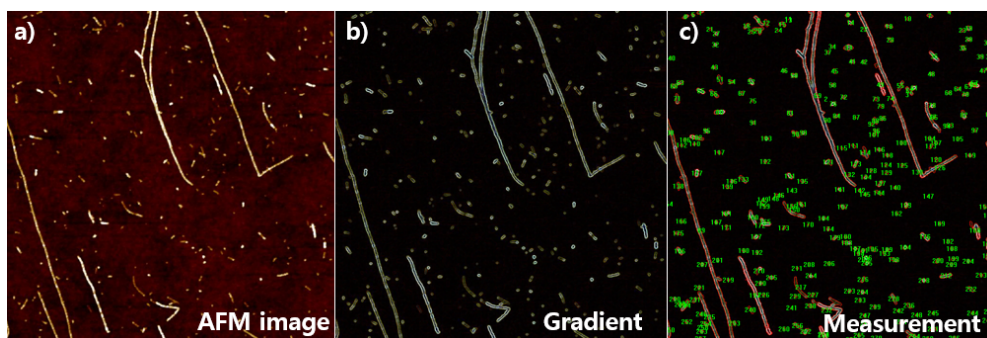


**Figure S5. Fibril length analysis from an AFM image by using a commercialized image processing software (i-Solution DT, IMT i-solution, Canada). a)** AFM image of the regrown fibrils with 1 wt% monomeric protein. **b)** Gradient image acquired by edge filter image processing. **c)** Length measurement of the decomposed and the regrown fibrils by using an image processing program.

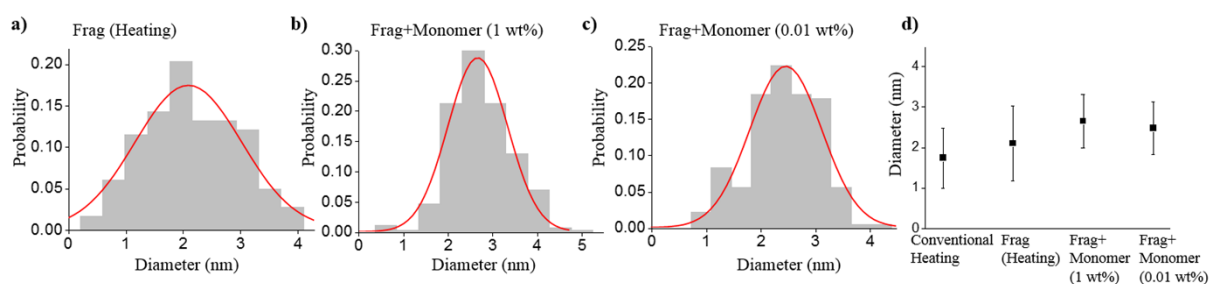


**Figure S6. Histograms of the diameter distribution of the regrown fibrils. a-c)** Diameter distributions of the heat-treated samples of fragments only **(a)**, fragments with 1 wt% of monomeric protein **(b)**, and fragments with 0.01 wt% of monomeric protein **(c)**. **d)** Average diameter of the regrown fibrils.

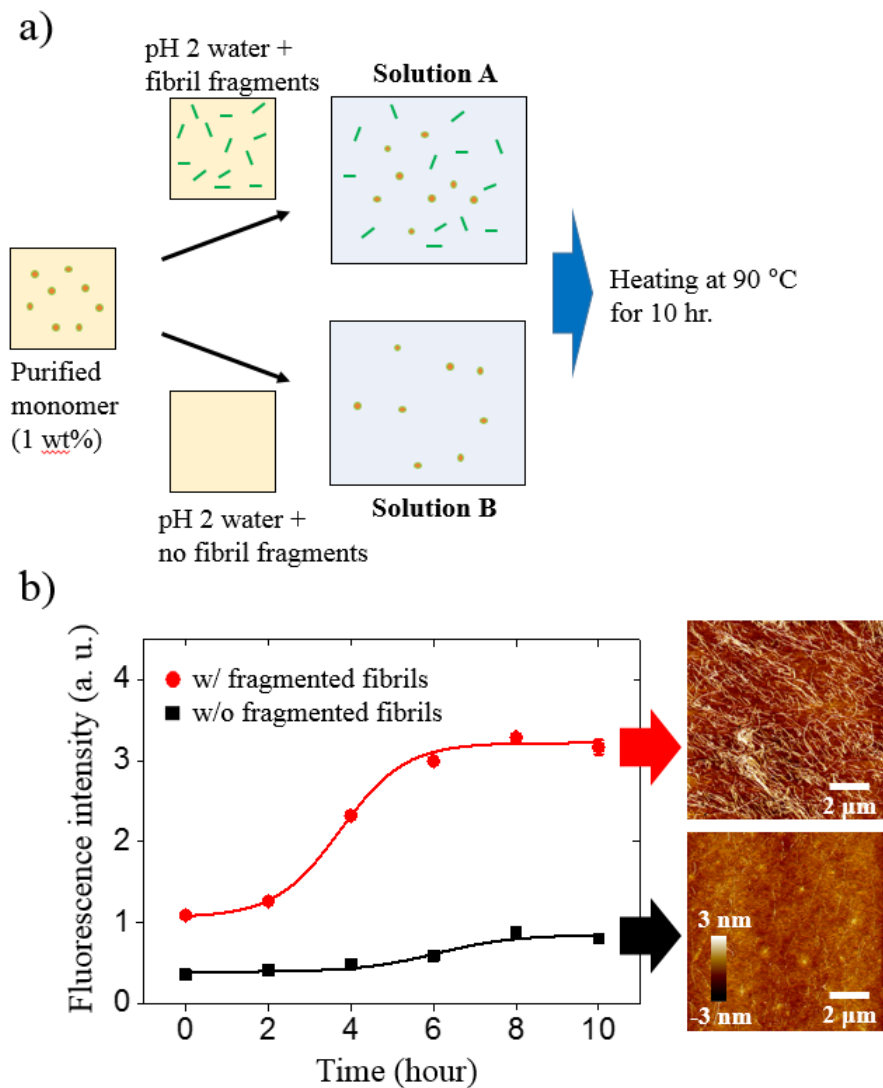


**Figure S7. Growth kinetics of the amyloid fibrils with addition of the fragmented fibrils.** a) A schematic of an experimental design to confirm whether the fibril regrowth mainly originated from the fragmented fibrils or from the additional monomer. Solution ‘A’ (8 ml) is a mixture (1:1) of monomer and fibril fragments (in pH 2 solution), and Solution ‘B’ (8 ml) is a mixture (1:1) of monomer and pH 2 solution not containing fibril fragments. b) Results of ThT assay and AFM analysis are consistent with previous works<sup>2,3</sup>.

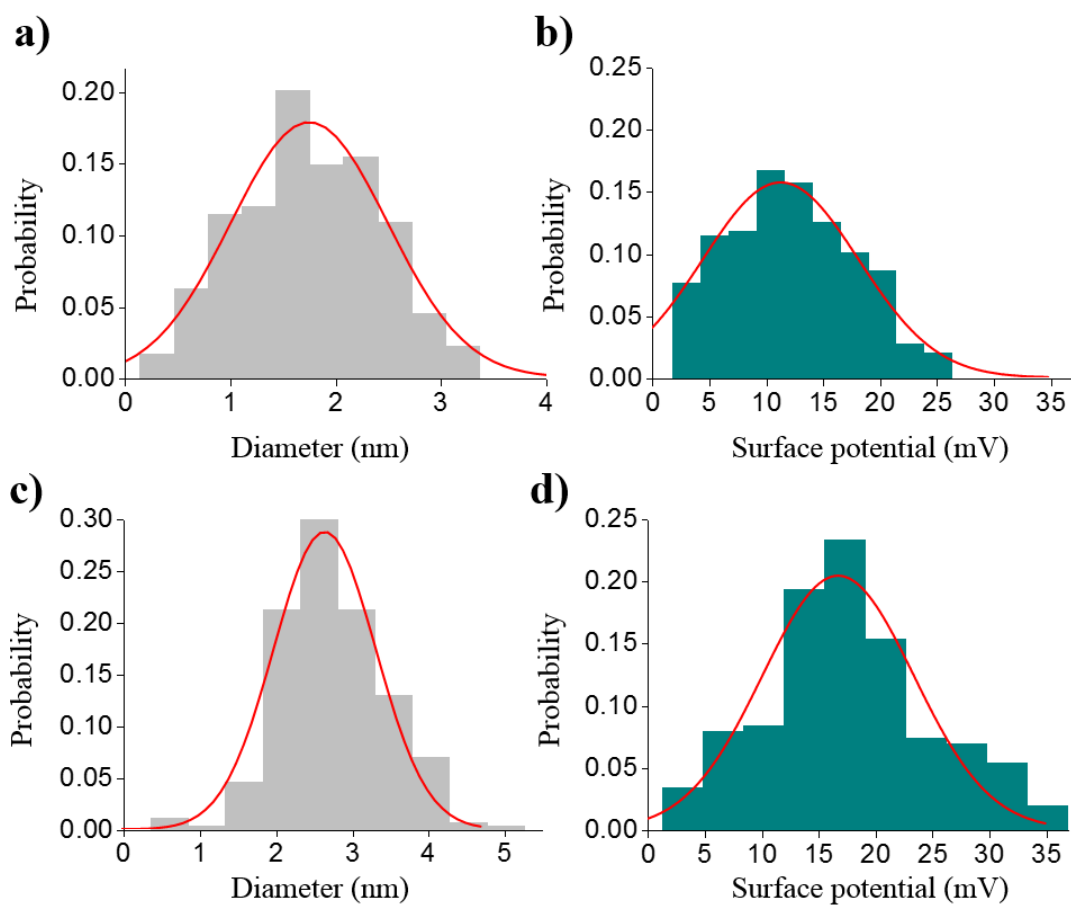


**Figure S8. Histograms of the fibril diameter and surface potential distribution of the original and the regrown fibrils.** Diameter distribution of the original fibrils **(a)** and the regrown fibrils with 1 wt% monomers **(c)**. Surface potential distribution of the original fibrils **(b)** and the regrown fibrils with 1 wt% monomers **(d)**.

## References

1. G. Lee, W. Lee, H. Lee, S. W. Lee, D. S. Yoon, K. Eom and T. Kwon, *Appl. Phys. Lett.*, 2012, 101, 043703-043704.
2. D. Pinotsi, A. K. Buell, C. Galvagnion, C. M. Dobson, G. S. Kaminski Schierle and C. F. Kaminski, *Nano Lett.*, 2013, 14, 339-345.
3. G. Merlini and V. Bellotti, *N. Engl. J. Med.*, 2003, 349, 583-596.